

Ion-beam-assisted fabrication and manipulation of metallic nanowires

N.S. Rajput^{1,2}, Z. Tong², H.C. Verma¹, X. Luo²

¹Department of Physics, Indian Institute of Technology Kanpur, Kanpur 208016, India

²Department of Design, Manufacture and Engineering Management, University of Strathclyde, Glasgow G1 1XQ, United Kingdom

E-mail: nitul2007@gmail.com

Published in Micro & Nano Letters; Received on 15th May 2014; Revised on 11th April 2015; Accepted on 13th April 2015

Metallic nanowires (NWs) are the key performers for future micro/nanodevices. The controlled manoeuvring and integration of such nanoscale entities are essential requirements. Presented is a discussion of a fabrication approach that combines chemical etching and ion beam milling to fabricate metallic NWs. The shape modification of the metallic NWs using ion beam irradiation (bending towards the ion beam side) is investigated. The bending effect of the NWs is observed to be instantaneous and permanent. The ion beam-assisted shape manoeuvre of the metallic structures is studied in the light of ion-induced vacancy formation and reconfiguration of the damaged layers. The manipulation method can be used for fabricating structures of desired shapes and aligning structures at a large scale. The controlled bending method of the metallic NWs also provides an understanding of the strain formation process in nanoscale metals.

1. Introduction: Nanowires (NWs) have a one-dimensional (1D) structure with various excellent size-dependent properties and have a wide range of applications, for example in sensor technology, nanoelectronics, energy, photonics, environmental technologies and so on. They (NWs) are recognised as the building blocks of the next generation micro/nanoelectronic devices [1–4]. Various fabrication techniques have been developed by several research groups to fabricate NWs [3–10]. However, compared to research on developing varieties of NWs, the extent of application-oriented research on NWs is limited. The reason could be the challenges encountered in handling and the integration of the nanoscale features with relatively larger units or devices.

In recent decades, various integration approaches have been proposed. Wu *et al.* [11] demonstrated an approach to grow organic NWs on Au coated areas through a surface energy-induced process. Patterned growth of the NW arrays and in-situ device integration were achieved by manipulating the Au electrode geometries. Peng *et al.* [12] developed a welding process for assembling nanoscale objects, where nanomanipulator probes were used to deposit a nanoscale volume of a predefined material by the Joule heating method. Moreover, direct manipulation of NWs using a nanomanipulator and an atomic force microscopy tip has also been carried out [13, 14]. The site-specific programmable growth technique to grow branched Si NWs, discussed by Jun and Jacobson [15], can lead to the development of a reliable nanoscale manoeuvre and integration technique. On the basis of the Bosch process, Arkan *et al.* [16] proposed another technique for the fabrication and integration of Si NWs with microscale metallic electrodes/contacts. These studies show a promising start in the development of manipulation and integration approaches for NWs with micron entities; however, to meet the challenges in designing future micro/nanoscale devices, it is necessary to develop a versatile, material independent and precisely controllable (with nanometric resolution) manipulating and integration method for NWs.

In this Letter, we present our work on an ion-induced shape modification process of metallic NWs. Although several popular and low-cost methods, such as template synthesis and electrospinning are available [4, 9, 10], we have implemented a different approach to creating the NWs. A combined process of chemical etching and ion beam milling has been used to fabricate metallic NWs. This fabrication approach has a unique advantage. The fabrication procedure during the ion beam milling can be monitored in

situ and thus the wire thickness can be easily controlled. The ion–matter interactions during the controlled shape modification of the metallic nanostructures are studied. The ion-beam-assisted shape modification [ion-induced manipulation (IIM)] method has potential application in fabricating structures of desired shapes as well as in assembling and editing micro/nanoelectronics.

The fabricated and manipulated NWs can be used in scanning probe microscopy (SPM) as a probe tip, where the resolution is often defined by the tip geometry. The high aspect ratio of the probe (i.e. the NW) can provide extra benefit in terms of examining the deep vertical structure without considerable artefacts. The metallic NWs can also be used as field emitting tips. The additional IIM process can provide the desired geometry easily.

2. Materials and methods: High-quality, corrosion resistant metallic wires (Heraeus make) were used for the experiment. The diameters of the wires were 17–40 μm . To thin down the wires from micron to nano dimensions, a two-stage step-by-step processing approach was used. Initially, the wires were thinned down to a few microns ($\sim 5 \mu\text{m}$) using specific chemical etching processes and further reduction to a few tens of nanometres was achieved using an ion beam milling process. These processes are discussed below.

2.1. Step I: chemical etching: The metallic wires (diameter: 17–40 μm) were taken and immersed in acid solutions to thin down the diameter. The etching solutions were prepared using commercially available chemical reagents (Rankem, RFCL Ltd). For etching Al wires (discussed in this Letter), a solution was prepared with the available HCl reagent, diluted with $\sim 60\%$ H_2O . The wires were kept in the etching solution to thin the wire diameter down to a few micrometres (Fig. 1). The thinned wires, feebly visualised by a naked eye, can be properly inspected using a scanning electron microscope (SEM). The thinned wires were held by fine tweezers and rinsed with deionised water for cleaning and for the removal of any unwanted substance from the wires' surfaces.

The part of a wire that was thinned down by the etching process was gently gripped using fine tweezers and one end of the wire was glued to an Al stub with the other end hanging freely. Conductive silver paint (Leitsilber 200, Ted Pella Inc.) was used to glue the wire to the stub which was kept in ambient air for ~ 5 min to dry out properly. The use of silver paint also ensures a proper electrical grounding of the wire (Fig. 1). Subsequently, the prepared sample (the wire along with the stub) was taken and placed inside a

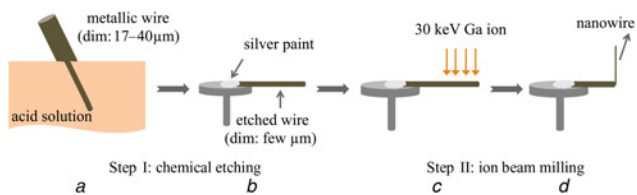


Figure 1 Schematic picture showing the steps to fabricate a metallic NW
a Metallic wire (diameter: 17–40 μm) is partially immersed in an acid solution for etching
b One end of the etched part of the wire (diameter about few micrometres) is glued with a metallic stub with the other end hanging freely
c Sample (metallic stub with the glued wire) is taken inside the FIB chamber and further irradiated by 30 keV Ga ions to thin down the wire
d Fabricated NW
 Structure makes a sharp angle with the rest because of the ion-induced bending process

focused ion beam (FIB) chamber for further thinning down of the wire.

2.2. Step II: ion beam milling: Dual-beam FIB systems (Nova 600 NanoLab and Nova 200 NanoLab, FEI make) were used for the experiments. The systems employ Ga liquid metal ion sources (LMISs) to produce a high-quality beam of singly charged Ga ions and Sirion-type field emission guns (FEGs) to generate high-resolution electron beams.

The free end of the wire was irradiated from the top direction with a high beam current of ~20 nA (applied beam voltage: 30 kV) as shown in Fig. 1*c*. Owing to the sputtering process (material removal because of the ion beam irradiation), the thickness of the wire became further reduced. As the wire became reduced to ~1 μm, the beam current was also reduced and set at 10–50 pA for fine milling. As the diameter of the wire became reduced further, the NW started moving towards the ion beam direction because of the ion-induced bending process (discussed in detail in the following Section) and produced a sharp angle with the rest to the unirradiated wire (Fig. 1*d*). Sputtering and bending using controlled irradiation resulted in the formation of a fine NW being fabricated at the edge of a relatively thicker wire.

3. Results and discussion: The SEM image of an Al NW fabricated using the above approach is shown in Fig. 2. The inset

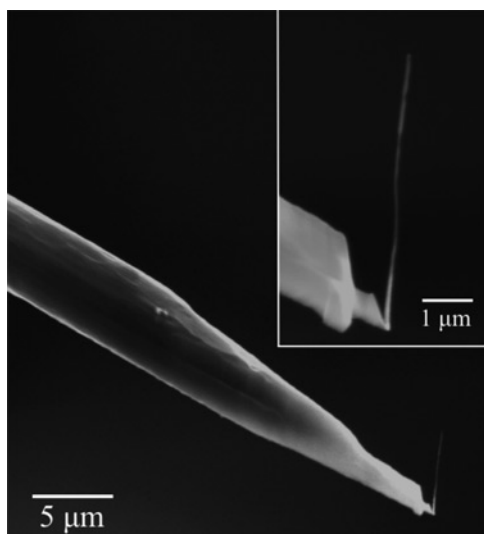


Figure 2 SEM image of an Al NW fabricated using a combined process of chemical etching and ion beam milling
 Inset shows a zoomed-in view of the fabricated structure

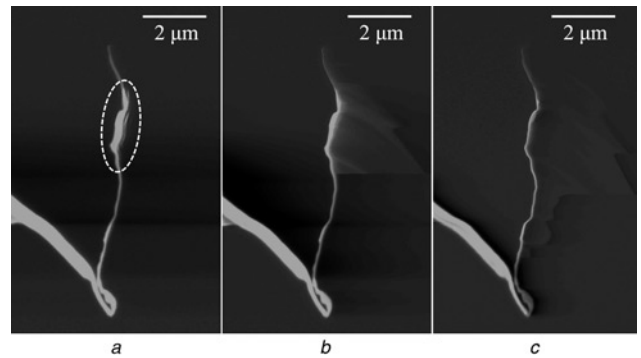


Figure 3 SEM images of an Al NW
 Applied beam voltage for the imaging was 15 kV
a Image was taken at the beam dwell time (t_d) of 100 ns
 Portion encircled with dotted line shows the charging effect
b Image was taken at $t_d = 1 \mu s$
c Image was taken at $t_d = 10 \mu s$

image shows the zoomed-in part of the fabricated NW. Even though the wire was fabricated from a high-quality Al wire, it is quite possible that after the ion beam irradiation the implantation of Ga ions and the creation of atomic defects could change the crystallinity of the wire.

The image in Fig. 2 was taken at 15 keV beam energy, 2.2×10^8 electrons $\mu m^{-2} s^{-1}$ beam flux and 100 ns beam dwell time. During the SEM scanning, charges can accumulate in the wire and may affect the SEM image formation process. As a result, the perception of the wire thickness and shape in the SEM image may differ from the actual size and shape. This is discussed in detail in the following Section.

3.1. Imaging and charging effect: Another example of a NW (Al) fabricated using the above-mentioned processes is shown in Fig. 3*a*. The diameter of the wire is ~25 nm. The NW has several curves in different portions of the structure. SEM images of the NW (Fig. 3) were taken at the applied beam voltage of 15 kV and beam flux of 1.9×10^8 electrons $\mu m^{-2} s^{-1}$. Fig. 3*a* was taken at a relatively low beam dwell time (t_d) of 100 ns. A bright region (the dotted portion in the image) appears in the image. The same NW imaged at a beam dwell time of 1 μs is shown in Fig. 3*b*. The bright layer seems to diminish in this case and nearly disappears when the beam dwell time was increased to 10 μs (Fig. 3*c*).

During the beam scanning, a large amount of charges will accumulate on the NW as it requires a finite amount of time (t_f) to become discharged through the base region of the NW and the sample stub. t_f depends on the amount of charge and the channel through which it becomes discharged, that is, the wire. Thus, the wire diameter can greatly affect the discharging process of the accumulated charges.

At the fast scanning mode (low t_d), when $t_d < t_f$, the accumulated charge had insufficient time to discharge and as a result the charging effect (the bright layer) appears in the wire (as shown in Fig. 3*a*). However, when the scanning speed was slowed down sufficiently, the accumulated charges had sufficient time to become discharged and as a result the bright region nearly disappears (Fig. 3*c*). The NW finally seems to have a uniform thickness throughout its length.

3.2. IIM and its mechanism: The fabricated metallic NW (Al) was subjected to a 30 keV Ga ion beam as illustrated in Fig. 4*a*. The irradiation was made at an incident angle of ~45° with the irradiated flux of 5.6×10^6 ions $\mu m^{-2} s^{-1}$. The arrow lines in the Figure show the direction of the ion beam irradiation. Figs. 4*b–d* show the SEM snapshots, taken after every 2–3 frames of ion

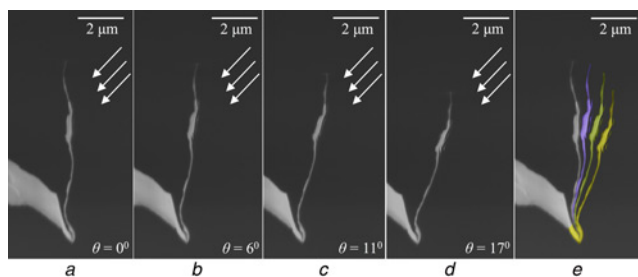


Figure 4 SEM images showing the bending process
a-d SEM images show the bending process of the metallic NW (Al NW) as a result of ion beam irradiation
 Arrows indicate the direction of the ion beam irradiation. Bending angle (θ) enunciates the deflection of the NW with respect to its initial position
e Overlapped images show the evolution of the irradiated NW

beam scanning. The snapshots show the gradual bending of the NW towards the ion beam direction. The deviation of the NW from its initial position is termed as θ and the measured values are shown in the Figures. The bending process is found to be instantaneous and permanent. The ‘permanent’ behaviour of the bending process infers the plastic nature of the process. The evolution of the bending process is shown in Fig. 4*e* by overlapping all the images (see Figs. 4*a-d*). Fig. 4*e* shows an important feature of the bending of the NW. The base part of the fabricated NW is found to bend considerably, compared to the other portions of the NW.

The ion-induced bending process has been observed by various groups in different nanoscale materials. The bending of a carbon nanotube [17], NWs [18–21], a carbon nanopillar [22], a biological structure [23], thin film structures [24], a metallic cantilever and so on [25] are reported and various mechanisms have been proposed to explain this nanoscale phenomenon. Some of the observed bending processes are discussed on the basis of ion-induced damage formation [17–19, 21, 24], whereas in a few materials the process has been discussed on the basis of the thermal stress developed during ion beam irradiation [22, 23].

To understand the bending phenomenon observed in metallic NWs, an atomistic investigation with the help of a Monte Carlo (MC) program was carried out. When an ion particle enters into the solid material, it interacts with the target atoms and transfers its energy and momentum to the nuclei and electrons of the target atoms. As a result of the collision process, large amounts of voids are produced within the interaction region. The interaction process also causes some surface atoms to come out of the material. The amount of voids (vacancies) and sputtering yield highly depend

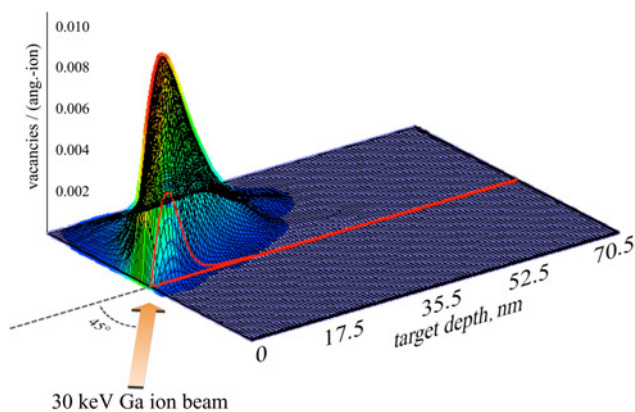


Figure 5 Shows the 3D vacancy profile in Al material created by 30 keV Ga ions irradiated at 45°

on the incident beam energy, incident angle, the beam type and the target material [26]. In addition to the surface damage and sputtering of the surface atoms, the Ga ions are likely to be doped in the NW. The volumetric change in the NW because of this implantation may be thought to initiate the bending process. To bend the NW towards the ion beam side, a heavy amount of Ga ions should be implanted on the opposite side of the NWs. The range of the implanted Ga ions irradiated at 45° in the Al NW, calculated by SRIM [27] (an MC-based program) is about 15 nm (whereas the diameter of the NW is ~ 25 nm). So a heavy concentration of implanted Ga ions on the rear surface is unlikely. Moreover, as the NW gradually bends, the bending angle (θ) increases and the implantation depth decreases [27]. Despite the changes in the implantation ranges of the Ga ions in the NW with θ , the wire bends towards the beam direction. Irradiating with low energetic Ga ions on a NW (where the implantation depth is much lower than the wire diameter) also shows bending of the NW towards the ion beam side. The experiments carried out on relatively thicker NWs also showed the typical bending of the NWs towards the ion beam side. These observations suggest that the volumetric change caused by the implantation has no significant role in the bending process of these structures.

SRIM results show that irradiating 30 keV Ga ions at an incident angle of 45° on the Al substrate can create vacancies of ~ 326 per ion and surface sputtering of ~ 9 atoms ion⁻¹. The Kinchin-Pease model was used to calculate the damage. The vacancies are created mostly at the surface level, within ~ 15 nm from the sample surface as shown in Fig. 5. Thus, a large number of vacancies and defects are created at the surface layers facing the ion beam. The disturbed/perturbed atoms at the surface layers tend to settle down in a much more stable configuration through a reconfiguration process.

The ion beam can also produce a significant amount of heat, which can accelerate the reconfiguration process. MC calculation shows that during the interaction of 30 keV Ga ions with the Al substrate irradiated at 45° incident angle, $\sim 65\%$ of the ion beam energy is converted into phonon generation, mostly contributed by the recoils [27]. Thus, a single ion can raise the temperature to $\sim 350^\circ\text{C}$ within the interaction region. A fraction of heat will be added from the ionisation process as well. As a result, the final temperature is expected to be more than this value. With the subsequent ion beam irradiation, the net temperature is likely to increase. However, there is also dissipation of heat through conduction and radiation. As a result of the dynamic process of heat generation by the ion irradiation and dissipation through conduction and radiation, an equilibrium temperature would be maintained. To calculate the saturated heat precisely, a proper nanoscale heat transport mechanism has to be developed. However, as the preliminary calculation enunciates (raise of temperature to $\sim 350^\circ\text{C}$ within the interaction region by a single ion), the temperature raised by the ion beam within the collision cascade region is sufficient to initiate the recrystallisation process in the NW [28].

As a result of the reconfiguration process, different amounts of stresses are developed across the layers of the system. Fig. 6 shows the formation of stresses in the NW as a result of the ion beam irradiation. When the surface layers facing the ion beam (L1) shrink in order to release the stress, this will subsequently affect the connected neighbouring layers (layers, L2, which are not receiving ion beam irradiation, but connected to L1 layers through the atomic bonds) and a new equilibrium shape is achieved with the structure bending towards the ion beam direction. Fig. 6 shows the schematic representation of the bending process; it also describes the process of ion beam irradiation, the subsequent development of compressive and tensile stresses across the surface layers and the bending of the NW.

The amount of damage formation and the reconfiguration process in a NW depends on the amount of irradiation received, the irradiation angle as well as the size of the structure; thus, the bending

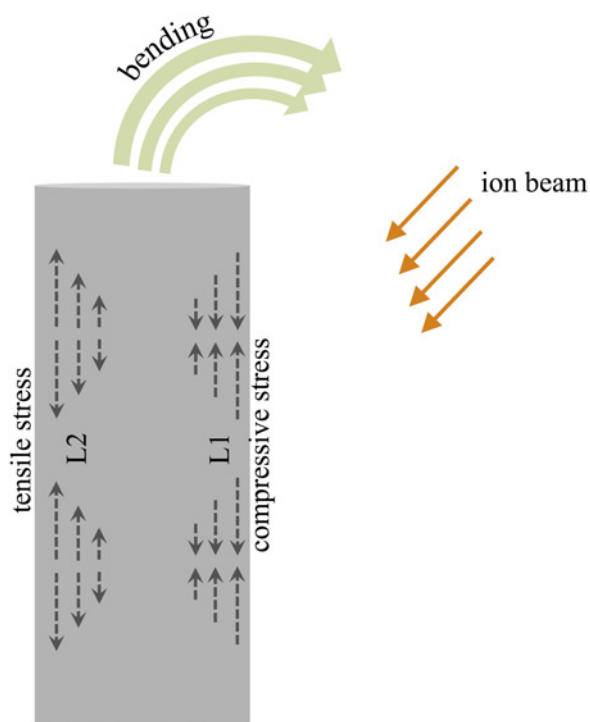


Figure 6 Schematic diagram showing the development of compressive and tensile stress as a result of ion beam irradiation and subsequent bending of the NW

tendency (an outcome of damage formation and recrystallisation) of an irradiated structure also depends of these parameters. Owing to several curves in the NW (Fig. 4), the NW receives ununiformed irradiation throughout its surface. The base portion might have received relatively larger irradiation (because of its geometry) causing a higher tendency of bending and, as a result, bending at the base region is comparatively higher than other portions. Owing to the uneven reception of irradiation by the NW throughout its length, the amount of curvatures also gradually decreases.

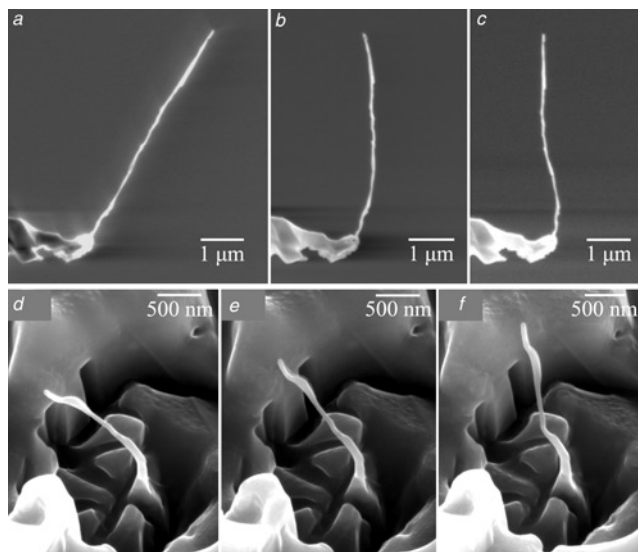


Figure 7 SEM images of Cu and Al NWs
a–c SEM snapshots showing the bending of a Cu NW during the ion beam irradiation from the top direction
d–f SEM images showing the bending of an Al NW while irradiated by the 16 keV Ga ion beam
 Irradiation was made from the top direction

The dynamic process of the ion-beam-induced damage formation and heat generation, dissipation of the heat, subsequent reconfiguration of the damaged layers and stress development across the layers requires a broader theoretical modelling to quantify the bending process precisely. Further theoretical investigation on the IIM process will be undertaken in a future project.

3.3. IIM in other systems: A few Cu NWs were fabricated using the same fabrication approach discussed in this Letter. Subsequently, the fabricated NWs were exposed to the high energetic Ga ions at a particular incidence angle. Similar patterns of bending are also observed in this case. The shape modification of a Cu NW during the 30 keV Ga ion beam irradiation is shown in Figs. 7*a–c*. The irradiation was made from the top direction.

Further, the top-down fabrication approach in FIB processing (ion beam milling) was used to fabricate Al NWs out of an Al substrate. The SEM image of an Al NW fabricated using this approach is shown in Fig. 7*d*. The bending of the Al NW towards the side of the ion beam during the 16 keV ion beam irradiation is shown in Figs. 7*d–f*.

It is observed that bending is more pronounced wherever there is a change in the wire thickness (Figs. 7*d–f*) compared to the straighter portions of the wire. This could be because of the fact that at these portions the local irradiation angle is suitable for creating the maximum amount of defects, which could lead to the generation of a higher amount of stress and hence a higher bending tendency. The primary role of the ion-induced temperature is expected to be only in the recrystallisation process of the NW material. In the case of NWs of varying thickness, the temperature distribution and diffusion along the NW would be inhomogeneous and hence the recrystallisation process would be ununiformed. This is also likely to play a key role in the ununiformed bending tendency along the NW.

Detailed investigation of the dependence of bending affinity on NW material is not investigated in this Letter. However, from the understanding of the bending phenomenon which we explain on the basis of defect formation, the reconfiguration process of the damaged layers and stress generation in the system, it can be argued that even though the same amount of doses are provided to different NWs, the bending affinity would be different in different NWs.

Experimental observations and our discussion enunciate that the ion-induced bending phenomenon ought to be a generic process for nanoscale crystalline/polycrystalline materials. This suggests that the IIM technique is also applicable to other nanoscale non-metallic crystalline materials.

4. Conclusion: A fabrication process that combines chemical etching and ion beam milling, to fabricate metallic NWs is introduced in this Letter. The NWs show a tendency of bending towards the ion beam side during the ion beam irradiation. The bending phenomenon is studied on the basis of vacancy formation and reconfiguration of the damaged layers, stress formation and releasing the stress through reshaping the structure. Our studies also show the generic nature of the IIM process in crystalline nanoscale structures and provide an understanding of the strain formation process in nanoscale metals.

The IIM process is instantaneous and permanent and with controlled doses the NWs can be precisely manipulated. This opens up the feasibility of using IIM as a versatile, material-independent manipulating and assembling method. The technique can find potential applications in different branches of nanotechnology. In photonics, for example, nanopillars are grown at a large scale to study the efficiency of metamaterials and it is seen that the efficiency depends on the angle made by the pillars with the surface. IIM, which can be used in aligning nanopillars at a large scale, can be very useful in such studies. In SEM/transmission electron microscope (TEM) systems, IIM can be useful in manoeuvring structures selectively.

5. Acknowledgments: The authors acknowledge the technical support provided by the staff at the Ion Beam Lab, IIT Kanpur and the Kelvin Nanocharacterization Centre, University of Glasgow. The authors are grateful to the NSTI, the Department of Science and Technology, India, IIT Kanpur, and the EPSRC (EP/K018345/1), UK, for financial support.

6 References

- [1] Li Y., Qian F., Xiang J., Lieber C.M.: 'Nanowire electronic and optoelectronic devices', *Mater. Today*, 2006, **9**, pp. 18–27
- [2] Duan X., Huang Y., Cui Y., Wang J., Lieber C.M.: 'Indium phosphide nanowires as building blocks for nanoscale electronic and optoelectronic devices', *Nature*, 2001, **409**, pp. 66–69
- [3] Keating C.D., Natan M.J.: 'Striped metal nanowires as building blocks and optical tags', *Adv. Mater.*, 2003, **15**, pp. 451–454
- [4] Khalil A., Lalia B.S., Hashaikheh R., Khraisheh M.: 'Electrospun metallic nanowires: synthesis, characterization, and applications', *J. Appl. Phys.*, 2013, **114**, p. 16, article id 171301
- [5] Dixon C.J., Curtines O.W.: 'Nanotechnology: nanofabrication, patterning and self assembly' (Nova Science Publishers, Inc., New York, 2010), pp. 237–293, 309
- [6] Wang Z.L.: 'Nanowires and nanobelts: materials, properties and devices – nanowires and nanobelts of functional materials' (Springer, New York, 2006), pp. 21–83, 93
- [7] Wang H., Sun M., Ding K., Hill M.T., Ning C.: 'A top-down approach to fabrication of high quality vertical heterostructure nanowire arrays', *Nano Lett.*, 2011, **11**, pp. 1646–1650
- [8] Burek M.J., Greer J.R.: 'Fabrication and microstructure control of nanoscale mechanical testing specimens via electron beam lithography and electroplating', *Nano Lett.*, 2010, **10**, pp. 69–76
- [9] Liu Y., Goebel J., Yin Y.: 'Templated synthesis of nanostructured materials', *Chem. Soc. Rev.*, 2013, **42**, pp. 2610–2653
- [10] Wang Y., Angelatos A.S., Caruso F.: 'Template synthesis of nanostructured materials via layer-by-layer assembly', *Chem. Mater.*, 2008, **20**, pp. 848–858
- [11] Wu Y., Zhang X., Pan H., Deng W., Zhang X., Zhang X., Jie J.: 'In-situ device integration of large-area patterned organic nanowire arrays for high-performance optical sensors', *Sci. Rep.*, 2013, **3**, p. 8, article id 3248
- [12] Peng Y., Cullis T., Inkson B.: 'Bottom-up nanoconstruction by the welding of individual metallic nanoobjects using nanoscale solder', *Nano Lett.*, 2009, **9**, pp. 91–96
- [13] Conache G., Gray S., Bordag M., *ET AL.*: 'AFM-based manipulation of InAs nanowires', *J. Phys. Conf. Ser.*, 2008, **100**, p. 4, article id 052051
- [14] Peng Y., Luxmoore I., Forster M.D., Cullis A.G., Inkson B.J.: 'Nanomanipulation and electrical behaviour of a single gold nanowire using in-situ SEM-FIB-nanomanipulators', *J. Phys. Conf. Ser.*, 2008, **126**, p. 4, article id 012031
- [15] Jun K., Jacobson J.M.: 'Programmable growth of branched silicon nanowires using a focused ion beam', *Nano Lett.*, 2010, **10**, pp. 2777–2782
- [16] Arkan E.F., Sacchetto D., Yildiz I., Leblebici Y., Alaca B.E.: 'Monolithic integration of Si nanowires with metallic electrodes: NEMS resonator and switch applications', *J. Micromech. Microeng.*, 2011, **21**, p. 9, article id 125018
- [17] Park B.C., Jung K.Y., Song W.Y., O B., Ahn S.J.: 'Bending of a carbon nanotube in vacuum using a focused ion beam', *Adv. Mater.*, 2006, **18**, pp. 95–98
- [18] Romano L., Rudawski N.G., Holzworth M.R., Jones K.S., Choi S.G., Picraux S.T.: 'Nanoscale manipulation of Ge nanowires by ion irradiation', *J. Appl. Phys.*, 2009, **106**, p. 6, article id 114316
- [19] Borschel C., Spindler S., Lerosé D., *ET AL.*: 'Permanent bending and alignment of ZnO nanowires', *Nanotechnology*, 2011, **22**, p. 9, article id 185307
- [20] Jun K., Joo J., Jacobson J.M.: 'Focused ion beam-assisted bending of silicon nanowires for complex three dimensional structures', *J. Vac. Sci. Technol. B*, 2009, **27**, pp. 3043–3047
- [21] Rajput N.S., Tong Z., Luo X.: 'Investigation of ion induced bending mechanism for nanostructures', *Mater. Res. Express*, 2015, **2**, p. 8, article id 015002
- [22] Tripathi S.K., Shukla N., Dhamodaran S., Kulkarni V.N.: 'Controlled manipulation of carbon nanopillars and cantilevers by focused ion beam', *Nanotechnology*, 2008, **19**, p. 6, article id 205302
- [23] Gour N., Verma S.: 'Bending of peptide nanotubes by focused electron and ion beams', *Soft Matter*, 2009, **5**, pp. 1789–1791
- [24] Yoshida T., Nagao M., Kanemaru S.: 'Characteristics of ion-induced bending phenomenon', *Jpn. J. Appl. Phys.*, 2010, **49**, p. 5, article id 056501
- [25] Rajput N.S., Banerjee A., Verma H.C.: 'Electron- and ion-beam-induced maneuvering of nanostructures: phenomenon and applications', *Nanotechnology*, 2011, **22**, p. 7, article id 485302
- [26] Yao N.: 'Focused ion beam systems: basics and applications' (Cambridge University Press, New York, 2007), p. 31
- [27] Ziegler J.F., Ziegler M.D., Biersack J.P.: 'SRIM – the stopping and range of ions in matter (2010)', *Nucl. Instrum. Method B*, 2010, **268**, pp. 1818–1823
- [28] Totten G.E., MacKenzie D.S.: 'Handbook of aluminum: physical metallurgy and processes' (CRC Press, New York, 2003), Vol. 1, p. 220